Title
LARGE SOLID ANGLE BRAGG-CURVE SPECTROMETER

Author
McDonald, R.J.

Publication Date
1983-08-01

Lawrence Berkeley Laboratory

UNIVERSITY OF CALIFORNIA

Accelerator & Fusion Research Division

Submitted to Nuclear Instruments and Methods in Physics Research

LARGE SOLID ANGLE BRAGG-CURVE SPECTROMETER

R.J. McDonald, L.G. Sobotka, Z.Q. Yao,
G.J. Wozniak, and G. Guarino

August 1983

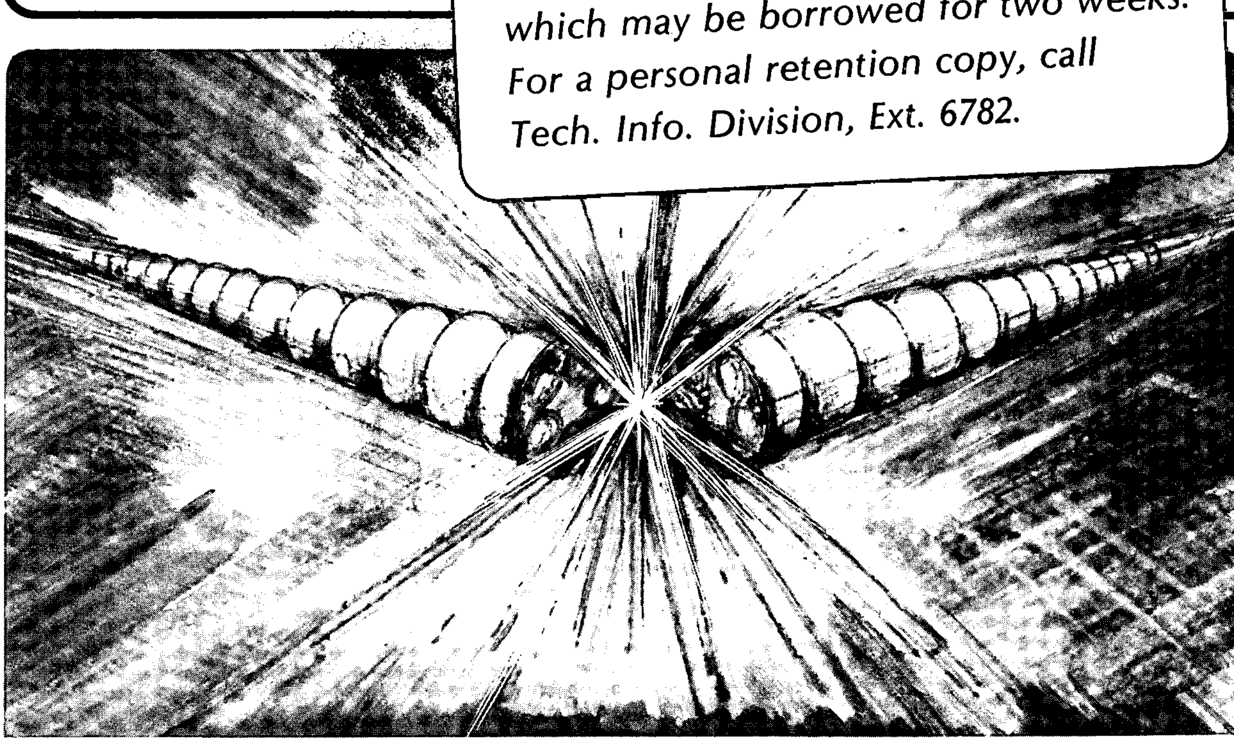

Prepared for the U.S. Department of Energy under Contract DE-AC03-76SF00098

DISCLAIMER

LARGE SOLID ANGLE BRAGG-CURVE SPECTROMETER*

R.J. McDonald, L.G. Sobotka, Z.Q. Yao[a)], G.J. Wozniak, and G. Guarino[b)]

Accelerator and Fusion Research and Nuclear Science Divisions

Lawrence Berkeley Laboratory

University of California

Berkeley, CA 94720

ABSTRACT

A conical Bragg-Curve Spectrometer (BCS) has been constructed. The outer case was a molded plastic cone. Printed circuit techniques were used to form an insert with inscribed equipotentials to approximate a $1/r^2$ electric field shape. The charge and energy resolution were measured for elastically scattered beams of 206 MeV ^{28}Si, 413 and 378 MeV ^{56}Fe, and 670 MeV ^{86}Kr ions. Performance of this detector, particularly its charge resolution, is discussed with respect to variation in solid angle.

---

a) Permanent address: Shanghai Institute of Nuclear Research, Shanghai, China.

b) Permanent address: Instituto di Fisica, Universita Degli Studi de Bari, 70100 Bari, Italy

1. Introduction

Recently, gas filled Frisch gridded ionization chambers have become increasingly utilized in heavy-ion nuclear reaction studies. These detectors provide excellent energy resolution, and, with a segmented anode, excellent Z-resolution. They are both radiation damage resistant and have a small pulse height defect relative to Si detectors. In addition, the detector thickness can be changed by simply changing the gas pressure. Conventional ionization chambers (ICs), with the electric field perpendicular to the ionization path, have been built in a variety of geometries with large solid angles.[1,2] Furthermore, these detectors have been made position sensitive in two dimensions. Position is determined in one direction by measuring the electron drift time to the Frisch grid; and in the other direction by either the addition of radial sense wires (theta grid) and delay-line readout[1] or a sawtooth anode configuration.[2]

In 1982, Gruhn et al.[3] demonstrated the viability of a gas-filled ionization chamber with the electric field parallel to the particle ionization track. This device was called a Bragg-curve spectrometer (BCS) because the time dependence of the ionization current collected at the anode contains information about the specific ionization along the track (the Bragg curve). For an ion stopping in the active volume (before the Frisch Grid) the total energy (E) can be obtained from the integral of the anode current, the atomic number (Z) is proportional to the maximum current (or Bragg peak), and the ion range (R) is proportional to the total width (in time) of the signal.

Within the last two years, several groups have built BCSs and studied their response to ions of $Z \leq 26$ at energies of several MeV per nucleon.[3–7] These detectors, all subtending small solid angles, gave results for energy and charge resolution comparable to what has been achieved for conventional ICs. The BCS, however, has the potential advantage that the Bragg peak (BP) should be independent of energy, thereby allowing one dimensional on-line monitoring of the Z resolution and simple Z gating. Although this has not been universally true in practice, a simple on-line transformation may be used to make Z independent of E over quite a wide range.[3]

Since the ionization current contains information about the specific ionization all along the track, digitizing the entire ionization signal might allow one to obtain better Z resolution and possibly A identification.[3] However, Asselineau et al.[4] have observed that the digitized anode signal differed from the calculated stopping-power values in the region of the Bragg peak; and Murakami et al.[5] have shown that for ions below 10 MeV per nucleon, the mass is a very weak function of the range, making A identification very difficult.

One application where a BCS should have a significant advantage over a conventional IC is in the construction of a modular 4π detection array where a compact geometry is required. Such an array, with good E and Z resolution (and possibly some additional position resolution) would be useful for a wide class of experiments. Several considerations need to be addressed regarding the feasibility of such a design: 1) Can a compact large solid angle BCS module be built with minimal dead area between modules? 2) Can the E and Z resolution of a small solid angle BCS be maintained in a large solid angle device? 3) Can such a device resolve events with Z > 26? These questions are addressed in the body of this paper.

2. Detector Construction

In order to obtain the close packing required for a modular 4π detector, the shape should be that of a frustrum of either a pyramid or a right circular cone. Our design utilizes this latter geometry. Charged particles emanating from a point source on the axis of this detector travel along radial paths. In order to maintain the desirable feature of having the particles travel along the field lines, a $1/r^2$ field is required in the detector volume. If the path of ionization deviates from the direction of the electric field lines, or the electron drift velocity is not constant, the ionization current measured at the anode is distorted. Thus, both the Bragg peak (Z) and range (R) information are affected. In any large solid angle BCS one must trade off or compromise on these criteria. A detector with a constant electric field E will produce a constant electron drift velocity, but the anode current will be distorted for ions that arrive at an angle to the direction of E. Choosing a field proportional to $1/r^2$ ideally eliminates this problem, but for most gases and detector dimensions of interest introduces a distortion due to the non-constant electron drift velocity. For our detector, we chose to use a $1/r^2$ field shape because we planned to make the detector position sensitive in future tests by either installing two sets of sense wires with delay-line read-out or by segmenting the anode. A true $1/r^2$ field was not achieved at either end of the detector due to the bulging window and planer Frisch grid and anode. In order to minimize the size of the detector and window it was placed close to the target (~10 cm). This close proximity of the detector to the target causes the reduced field (E/P) to change by about a factor of 10 between the cathode and grid.

The BCS was operated with a cathode potential of -4000V and a pressure of ~ 450 torr of P-10 (90% argon - 10% methane) gas. The maximum change in E/P causes the electron drift velocity to change by ~40% over a range corresponding to the stopping of ions with energies between 1-8 MeV/nucleon.[8,9] This variation in electron drift velocity is expected to have very little effect on the energy signal, and the greatest effect on the range signal.

Central to the construction of this detector was the use of computer aided design to produce a printed circuit insert containing a set of equipotentials on the inside of a frustrum of a right circular cone. The details of this construction are as follows: Circular copper stripes 0.2 cm wide and 0.05 cm apart were inscribed on a flat anulus of 0.01 cm thick G-10 material.[10] Resisters, 22 MΩ each, were attached to certain stripes to approximate a 1/r potential gradient. Thirteen such resistors were used. A thin line of resistive ink[11] connected all stripes to improve uniformity in the voltage gradient. The resistance along the ink path was kept large with respect to the 22 MΩ resistors. This flat anulus, when cut to intercept an arc of ~85°, folded, and placed inside the plastic housing as shown in fig. 1a, becomes a set of electrodes providing an approximate $1/r^2$ field. A Frisch grid made of 38 μm tungsten wire mesh, 16x16 per cm, and at a potential of 0 V, follows these electrodes. Its screening inefficiency was calculated[12] to be ~1%. The anode was 1.5 cm behind the Frisch grid. The 3.8 cm diameter window was constructed of 175 $\mu g/cm^2$ aluminized mylar supported by the same wire mesh used for the Frisch grid. This window was capable of supporting 500 torr. Figure 1b shows a section view of the detector and includes the important dimensions.

3. Experimental Results

The BCS was placed inside a 152 cm diameter scattering chamber with its window 10 cm from a 0.5 mg/cm^2 Au target. Beams of ^{28}Si, ^{56}Fe and ^{86}Kr were obtained from the Lawrence Berkeley Laboratory SuperHILAC. Aluminum collimators, on a separate movable table, defined acceptance angles of ±1.2° to ±9.3° as listed in Table 1. The current signal from the anode (maximum total width ~ 6 μs) passed through a charge sensitive preamplifier and was directed along three paths: 1) The total energy was obtained from a spectroscopy amplifier with an 8 μs shaping time, 2) the BP signal (Z) was obtained from an amplifier with a 0.8μs shaping time, and the width of the anode signal (range) was obtained by pulse-shape analysis as follows: A TAC was started by the signal from a constanct fraction discriminator and stopped by the zero crossing time from the bipolar output of the amplifier. All signals were collected event-by-event and stored on magnetic tape for subsequent off-line analysis.

The information contained in these signals is illustrated by figure 2 which shows data from simultaneous beams of 413 MeV ^{56}Fe and 206 MeV ^{28}Si scattered at 30° from a thin Ag target. Each spectrum shows two peaks, corresponding to the energy, atomic number, and range of elastically scattered Fe and Si. Figure 3 is even more illustrative of the operation of the BCS. These two dimensional scatter plots of (a) range versus energy and (b) range versus charge for the Fe + Ag and Si + Ag reactions show separate regions for the scattered Si and Fe particles. Note that Fig. 3b shows a strong dependence of the BP on the range for the Fe events. As mentioned in the introduction, a dependence of the height of the Bragg peak (Z) on energy (or range) has been observed. Some authors[3-6] have attributed this effect to a grid screening inefficiency, however, Schiessl et al.[7], attribute it to an excessively long shaping time constant of the BP amplifier. Either cause could produce this effect. Most of this energy dependence can be eliminated by a linear transformation of the raw BP signal:

$$BP' = BP - k * E$$

In order to optimize the mechanical and electrical parameters of the detector and to determine its best performance, data were obtained for the Fe+Au reaction at 35° in the lab using a ±1.2° opening angle in the detector. Figure 4 shows a two dimensional plot of the linearized BP signal versus energy for the reaction products. Note the excellent separation of adjacent elements in the region below Z = 26. As indicated in Table 2, this data yields a $\Delta Z/Z \approx 1.5$ and a $\Delta E/E$ of ~1% after subtraction of the kinematic contribution and the energy spread of the beam.

To test the effects of increasing solid angle on the detector performance, the acceptance angle was increased from 1.4 to 83 msr. Four measurement steps were taken for Fe- and two for Kr- induced reactions.

Figure 5 shows a collage of projections of the linearized BP signal for a narrow energy gate in the deep-inelastic region. For small solid angles, this detector gives Z-resolution comparable to that obtained by Gruhn et al.[3] When the solid angle is increased from 1.4 to 83 msr, $\Delta Z/Z$ only deteriorates from 1.5% to 1.9% FWHM. For the Kr data, individual elements are identified ($\Delta Z/Z < 2\%$) at both 5 and 83 msr. The Z-identification obtained with this detector is comparable to that obtained with conventional large solid angle ICs[13] and is quite acceptable for a large class of experiments. For this detector, it is not clear whether the small increase in $\Delta Z/Z$ as a function of solid angle depends on deviations from a true $1/r^2$ field, variations in electron drift velocity, or charge loss due to proximity with the detector wall.

4. Discussion and Future Improvements

A large solid angle Bragg-curve spectrometer which could serve as an element in a compact 4π detection array for heavy-ion nuclear physics experiments has been designed and tested. This detector is capable of identifying the charge and energy of Fe and Kr reaction products with $\Delta Z/Z < 2\%$ and $\Delta E/E \sim 1\%$ intrinsic resolution. Several compromises in the design were made to enhance performance at large solid angles. The Z-resolution could possibly be improved by giving more care to the field shape and minimizing variations of the electron drift velocity. For example, if a detector was built with the same depth (~23 cm) but located at 20 cm from the target, instead of 10 cm, the ratio of E/P would change by a factor of 5 rather than a factor of 10. Furthermore, the variation in electron drift velocity along the length of the detector could also be reduced by a better choice of gas and operating voltage.

To fully exploit the potential of a large solid angle BCS one needs to make the device position sensitive. This could be accomplished by placing a position sensitive avalanche detector in front of the BCS or by making the device intrinsically position sensitive. The latter could be accomplished either by installing two additional grids of sense wires and using a delay-line readout, or by segmenting the anode. A full discussion of these options is beyond the scope of this paper. While many questions concerning the BCS remain unanswered, the results presented in this paper suggest that continued efforts to investigate the potential of the BCS are warrented.

ACKNOWLEDGMENTS

The authors acknowledge valuable discussions with C. R. Gruhn and would like to thank R. Devries of Los Alamos National Laboratory for providing the conical shell used in constructing this BCS.

*This work was supported by the Director, Office of Energy Research, Office of High Energy and Nuclear Physics, Nuclear Division of the US Department of Energy under contract No. DE-AC03-76SF0098.

Table 1

Aperture Diameter	Opening Angle	Solid Angle
0.32 cm	± 1.2°	~ 1.4 msr
0.64 cm	± 2.3°	~ 5.1 msr
1.27 cm	± 4.7°	~ 21. msr
2.54 cm	± 9.3°	~ 83. msr
OPEN	±12.8°	~156 msr

Table 2

	Fe		Kr	
Solid Angle	ΔE/E (FWHM)	ΔZ/Z (FWHM)	ΔE/E (FWHM)	ΔZ/Z (FWHM)
1.4 msr	1%	1.5%	–	–
5.1 msr	–	1.7%	–	1.4%
21 msr	–	1.7%	–	–
83 msr	–	1.9%	–	1.7%

REFERENCES

1) H. Sann, H. Damjantschitsch, D. Hebbard, J. Junge, D. Pelte, B. Povh, D. Schwalm, and D.B. Tran Thoai, Nucl. Instr. and Meth. 124 (1975) 509.

2) G. Rosner, B. Heck, J. Pochodzalla, G. Hlawatsch, B. Kolb, and A. Miczaika, Nucl. Instr. and Meth. 188 (1981) 561.

3) C.R. Gruhn, M. Binimi, R. Legrain, R. Loveman, W. Pang, M. Roach, D.K. Scott, A. Shotter, T.J. Symons, J. Wouters and M. Zisman, R. Devries, Y.C. Peng, and W. Sondheim, Nucl. Instr. and Meth. 196 (1982) 33.

4) J. M. Asselineau, J. Duchon, M. L'Haridon, P. Mosrin, R. Regimbart and B. Tamain, Nucl. Inst. and Meth. 204 (1982) 109.

5) H. Ikezoe, Y. Tomita, N. Shikazono, and T. Murakami, Nucl. Inst. and Meth. 196 (1982) 215 and T. Murakami, H. Ikezoe, Y. Tomita and N. Shikazono, JAERI-M 9514, (1981).

6) G. D'Erasmo, D. Fabris, F. Gramegna, I. Iori, A. Moroni, G. Nebbia, A. Pantaleo, G. Prete, R. A. Ricci, G. Viesti, Progress Report of the INFL, Laboratori Nazionali di Legnaro, Italy.

7) Ch. Schiessl, W. Wagner, K. Hartel, P. Kienle, H.J. Körner, W. Mayer and K. E. Rehm, Nucl. Inst. and Meth. 192 (1982) 291.

8) L. G. Christophorou, D.L. McCorkle, D.V. Maxey and J. G. Carter, Nucl. Instr. and Meth. 163 (1979) 141.

9) L. C. Northcliff and R. F. Schilling, Nuclear Data A7, (1974), 1.

10) G-10: Norplex Divison, UOP, 300 Norplex Dr., La Crosse, WI, 54601.

11) Resistive Ink: 300 M Ω/Square; R300 M5 from: Micro-Circuits Co.,Electronic Products for Research and Industry, Route 1, Box 518 New Buffalo, MI 49117.

12) O. Bunemann, T. E. Cranshaw, and J. A. Harvey, Canadian Journal of Research 27A (1949) 191-206.

13) G. Rudolf, A. Gobbi, H. Stelzer, U. Lynen, A. Olmi, H. Sann, R.G. Stokstad and D. Pelte, Nucl. Phys. A330 (1979) 243.

Figure Captions

Fig. 1 (a) "Exploded" view of the conical BCS showing its major components.

(b) Section of the BCS showing its significant dimensions.

Fig. 2) Signals derived from the anode current of the BCS for simulaneous beams of 206 MeV ^{28}Si and 413 MeV ^{56}Fe scattered at 30° from a 0.5 mg/cm^2 Ag target: (1) Energy, (2) Bragg peak (Z), and (3) Range. For this measurement a 0.9 mg/cm^2 polycarbonate window was used on the BCS.

Fig. 3) (a) Scatter plot of range vs energy and (b) range vs charge for simultaneous beams of Fe and Si (See figure 2).

Fig. 4) Two dimensional plot of the linearized Bragg peak as a function of energy for ^{56}Fe ions scattered at 40° from 0.5 mg/cm^2 Au target with a 1.4 msr acceptance angle. The detector window was 175 μg/cm^2 aluminized mylar.

Fig. 5) Projections of the linearized Bragg peak for a narrow energy gate in the deep-inelastic region. This demonstrates the charge resolution of the detector for increasing solid angle (see Table 2).

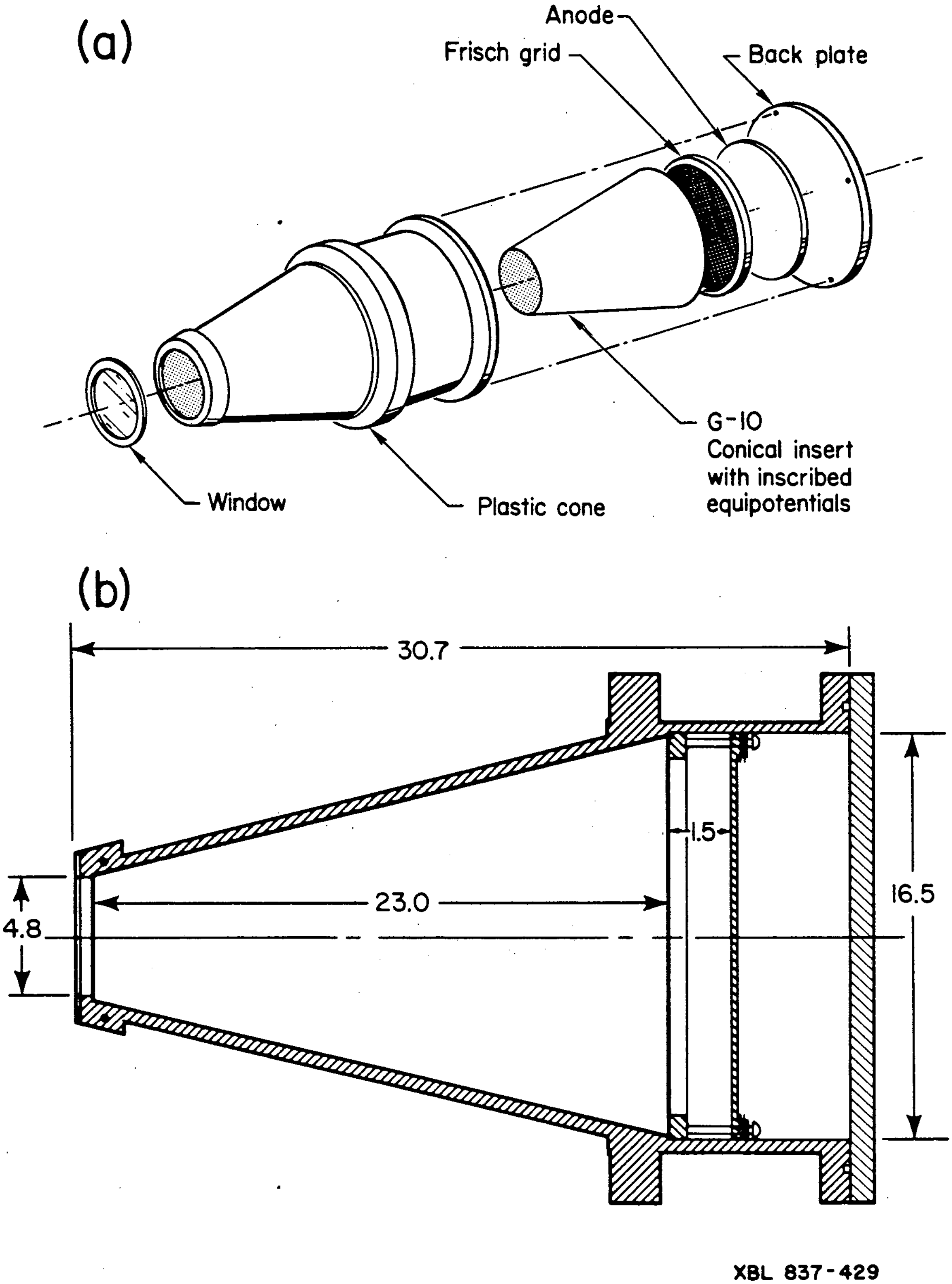
(a)
Anode
Frisch grid
Back plate
G-10
Conical insert
with inscribed
equipotentials
Window
Plastic cone
(b)
30.7
1.5
23.0
16.5
4.8
XBL 837-429

Fig. 1

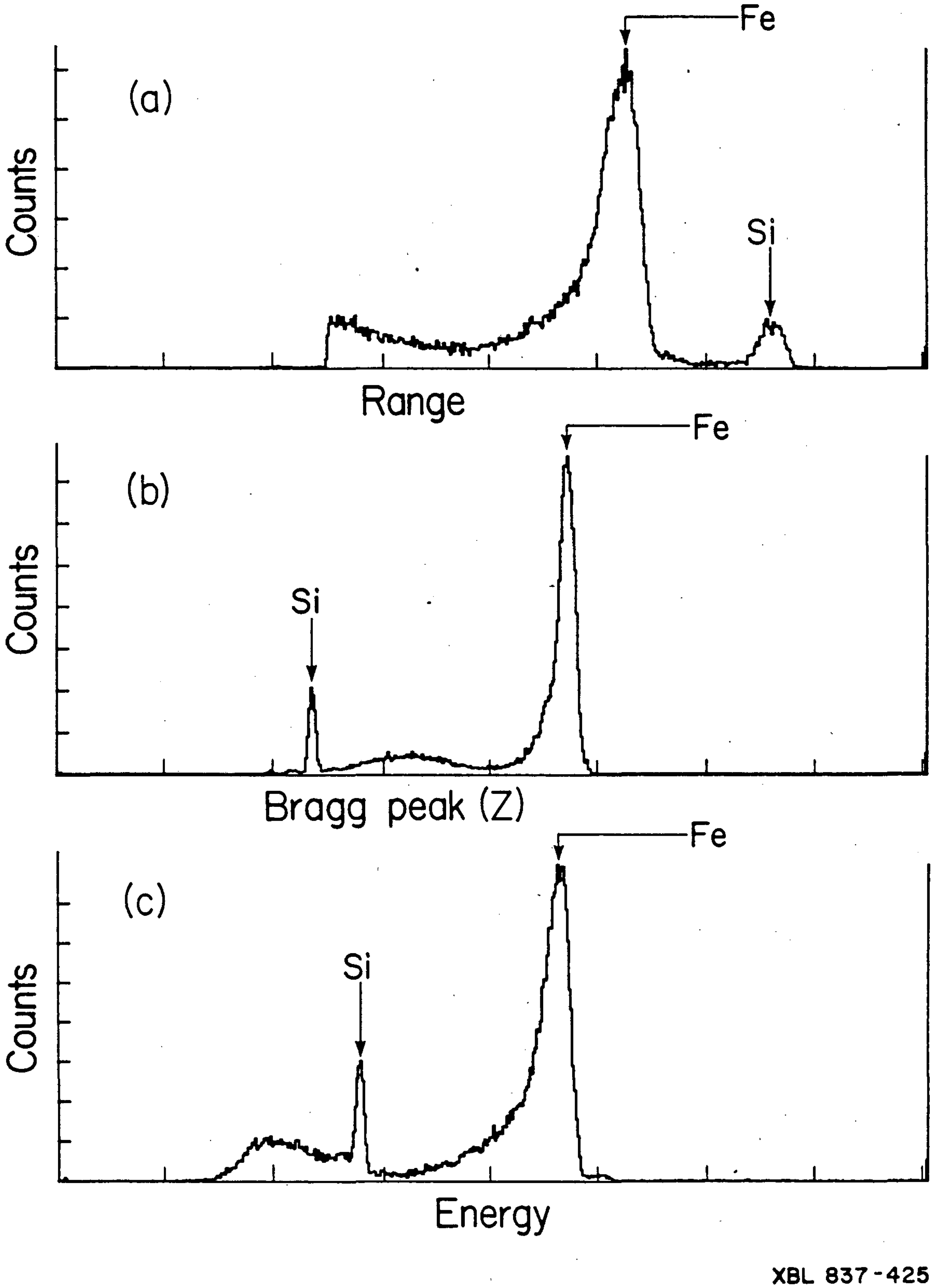
Fe
(a)
Counts
Si
Range
Fe
(b)
Counts
Si
Bragg peak (Z)
Fe
(c)
Counts
Si
Energy
XBL 837-425

Fig. 2

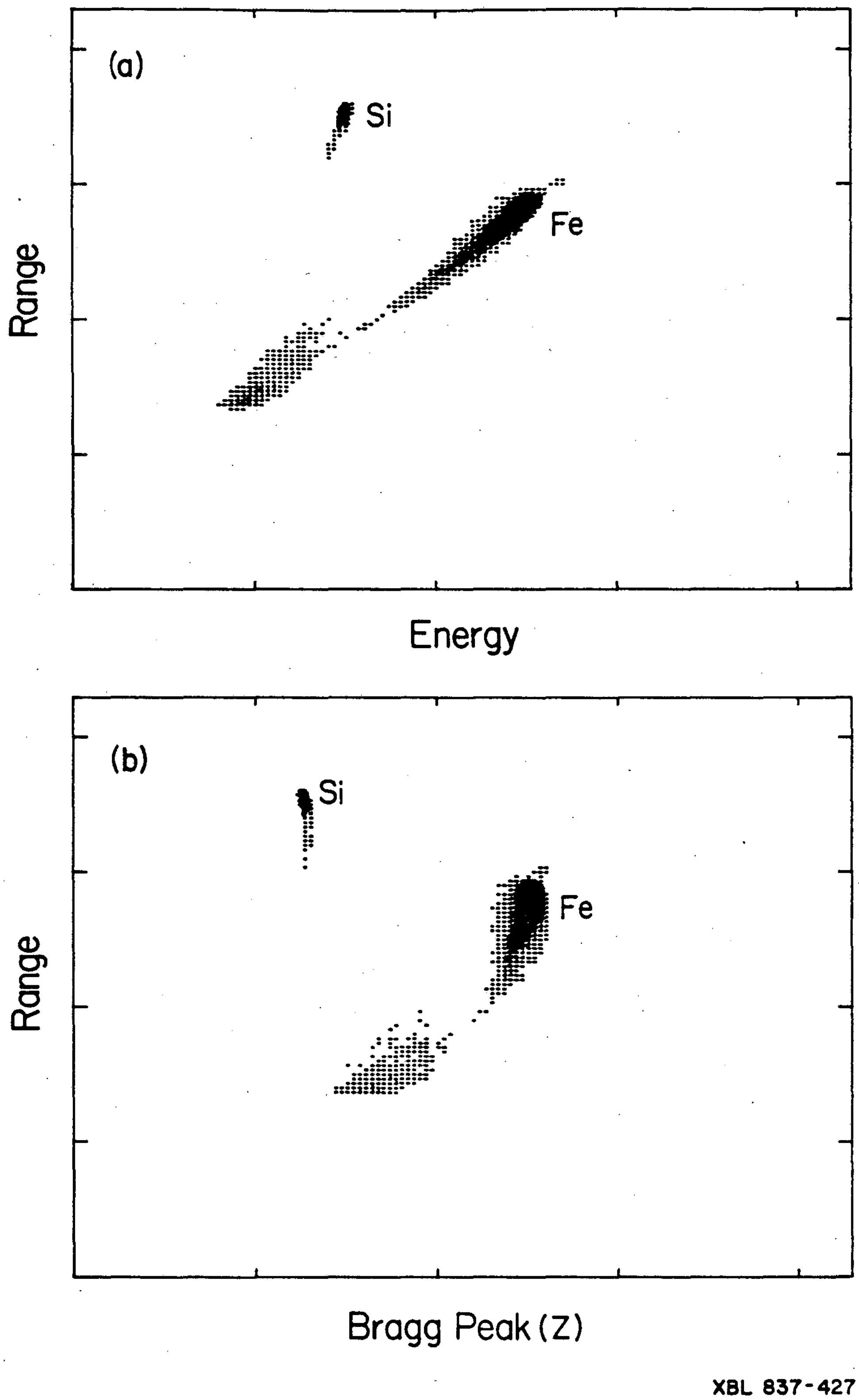

Fig. 3

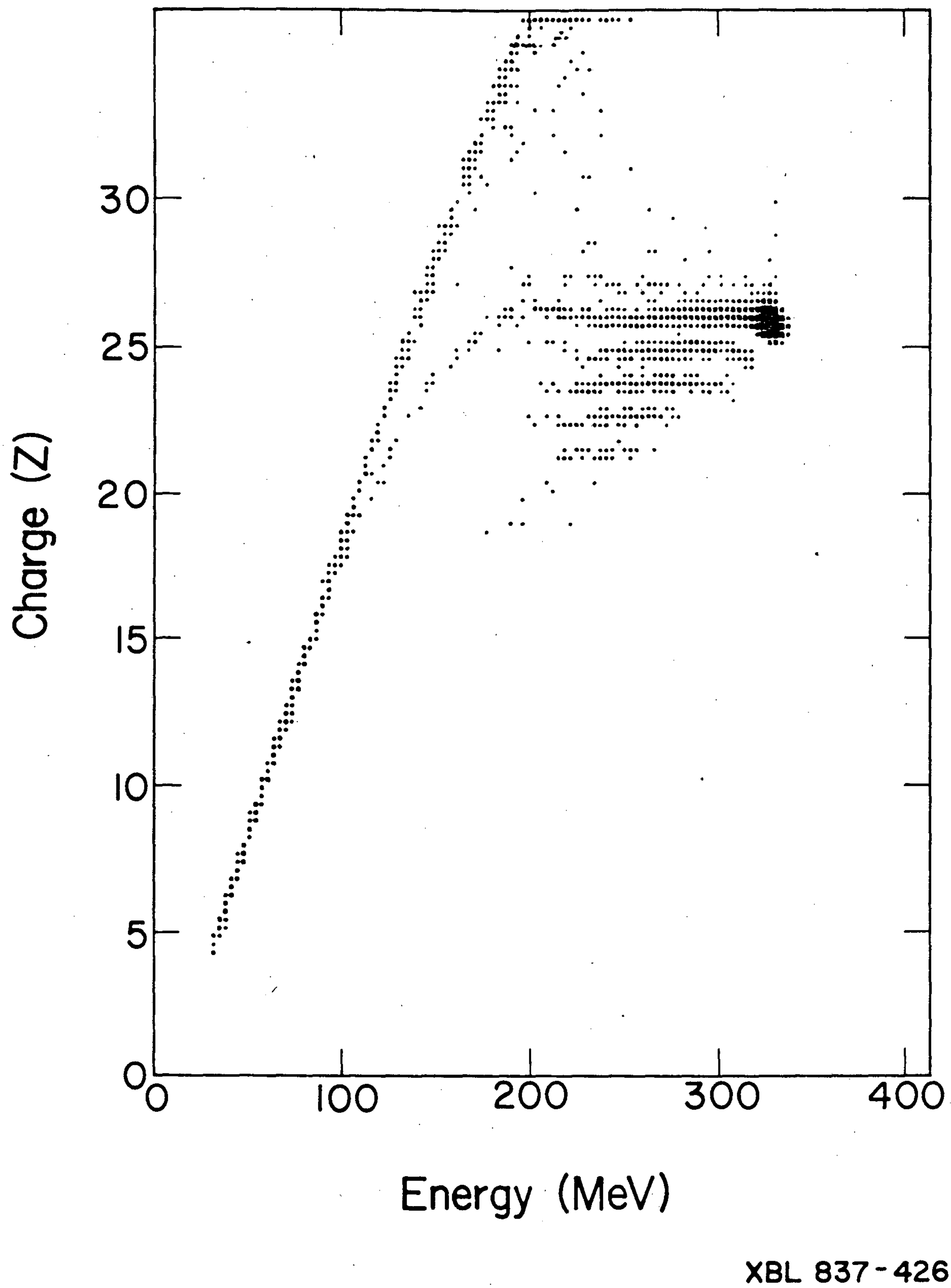

Charge (Z)
0
5
10
15
20
25
30
0
100
200
300
400
Energy (MeV)
XBL 837-426

Fig. 4

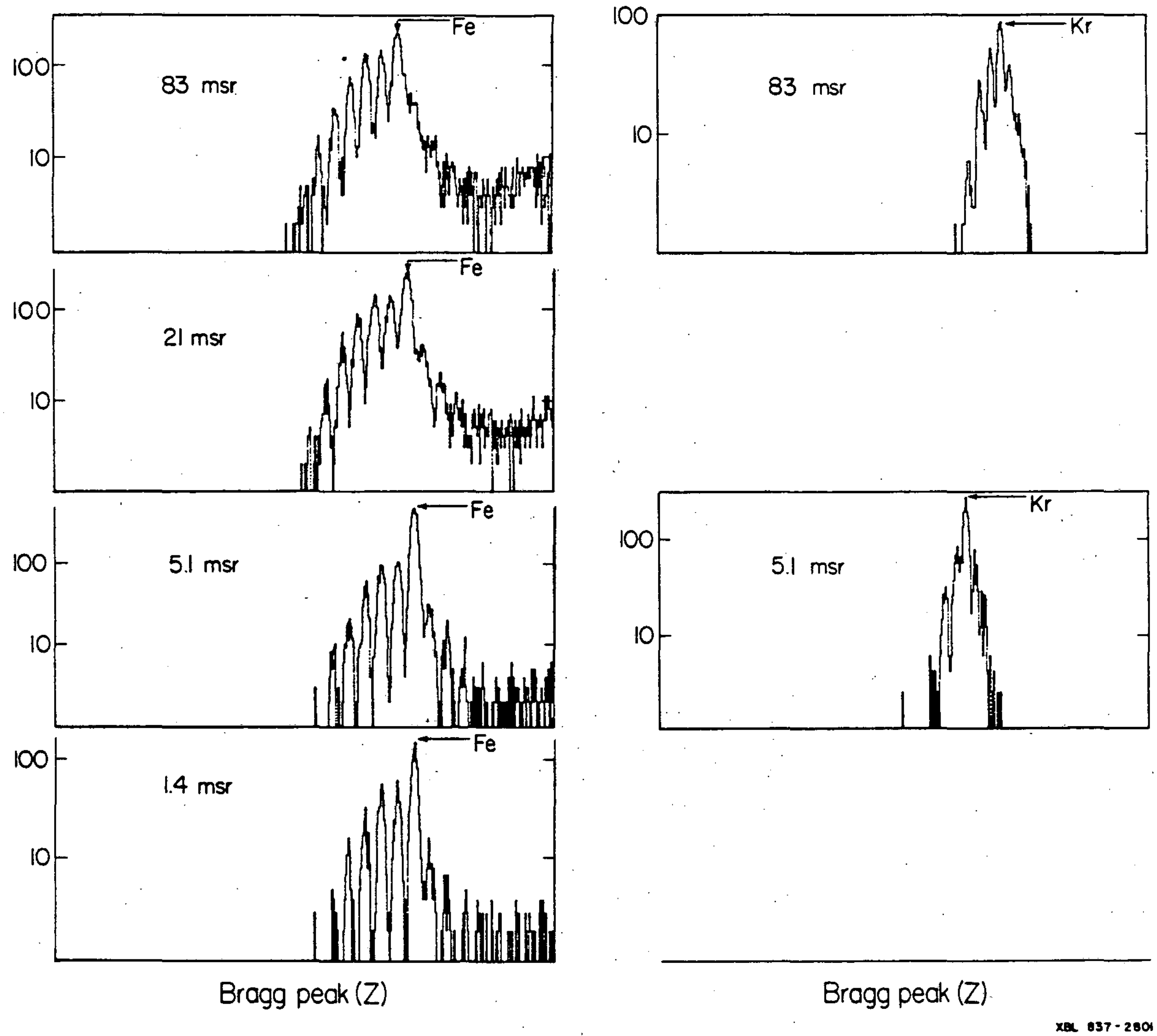
Fe
100
83 msr
10
Fe
100
21 msr
10
Fe
100
5.1 msr
10
Fe
100
1.4 msr
10
Bragg peak (Z)
100
Kr
83 msr
10
Kr
100
5.1 msr
10
Bragg peak (Z)
XBL 837-2801

Fig. 5

TECHNICAL INFORMATION DEPARTMENT
LAWRENCE BERKELEY LABORATORY
UNIVERSITY OF CALIFORNIA
BERKELEY, CALIFORNIA 94720